



Cite this: *Green Chem.*, 2014, **16**, 4371

Ultrafinely dispersed Pd nanoparticles on a CN@MgO hybrid as a bifunctional catalyst for upgrading bioderived compounds†

Mingming Li, Xuan Xu, Yutong Gong, Zhongzhe Wei, Zhaoyin Hou, Haoran Li and Yong Wang*

A novel and sustainable synthesis of a Pd/CN@MgO catalyst is presented here, offering a bifunctional catalyst with high catalytic activity towards a tandem aldol condensation–hydrogenation reaction of furfural with acetone in a one-pot reactor. The incorporation of biomass based hydrophilic N-containing carbon (CN) in the catalyst provides a subtle but elegant method to control the good water dispersibility, the reaction stability, and the ultrafine dispersion of palladium particles (2.2 nm in average size) in the bifunctional catalyst Pd/CN@MgO. With such improved features, an impressive 99% furfural conversion and 95% selectivity for the hydrogenated products (saturated ketones) was obtained by using Pd/CN@MgO as a novel bifunctional catalyst in the reported tandem reaction. This catalyst design strategy and the high efficiency of the catalyst in the reported system offer potential for the preparation of bi/multifunctional catalysts and the one-pot synthesis of bioderived intermediates.

Received 9th May 2014,
Accepted 23rd June 2014
DOI: 10.1039/c4gc00850b
www.rsc.org/greenchem

Introduction

Heterogeneous catalysts, with the advantage of being easily separated from the reactants and products of the overall catalytic process, have been an appealing research topic in recent years.¹ As the selection of heterogeneous catalysts offers special challenges, much effort has been focused on the design and synthesis of new efficient, simple, and sustainable materials as catalysts or catalyst supports.

Among the various heterogeneous catalysts, supported catalysts are frequently used. In particular, the catalysts supports play significant roles in their reaction performance. Among the various supports, metal oxides (*e.g.* Al₂O₃, MgO, ZrO₂, CeO₂ and SiO₂),^{2–5} zeolites,⁶ metal–organic frameworks (MOFs)^{7,8} and carbons (including carbon black, activated carbon, graphene, carbon nanofibers, carbon nanotubes, and carbon spheres)^{9–14} are frequently used. However, these catalyst supports may suffer from problems like non-uniform particle size with poor dispersion, weak particle–support bonding, poor water dispersibility, or reaction monofunctionality. Intriguingly, recent years have witnessed increased interest in developing hybrids as catalyst supports with enhanced cata-

lytic performance.^{15–18} Notably, bifunctional or multifunctional catalysts that have the advantage of simplifying reaction processes without the requirement of dealing with the separation or treatment procedures of the individual operations,¹⁹ have recently attracted intensive studies.^{18,20,21} Therefore, developing novel bifunctional catalysts with enhanced catalytic activity is desirable.

Biomass, as a green, sustainable and cheap resource easily available in nature, can be directly converted into various kinds of carbon-based materials.^{22–24} Recently, an intriguing method of incorporating nitrogen into the structure of carbon materials has gained increasing interest, as some beneficial effects on the physicochemical properties of the materials, including the electrical conductivity, basicity, and obvious modifications and enhancements of the catalytic activity, have been demonstrated.^{25–27} The presence of doped nitrogen heteroatoms on carbon supports has been shown to stabilize noble metal (*e.g.* Pd, Pt) NPs due to the activation of neighboring carbon atoms caused by the electron affinity of nitrogen,^{28,29} which is rather beneficial for heterogeneous catalysts.³⁰ Recently, much of our work has focussed on developing N-containing carbon supported catalysts, and satisfying results were obtained.^{10,14,31–33} However, as they are relatively neutral, these N-containing carbon supported catalysts are restricted to monofunctionality. The heterogeneous basic MgO catalyst, with its ability to trigger certain reactions like condensation reactions,^{18,34} has been widely studied, but problems have been encountered such as inferior hydrothermal stability

Carbon Nano Materials Group, ZJU-NHU United R&D Center, Department of Chemistry, Zhejiang University, Hangzhou 310028, P. R. China.

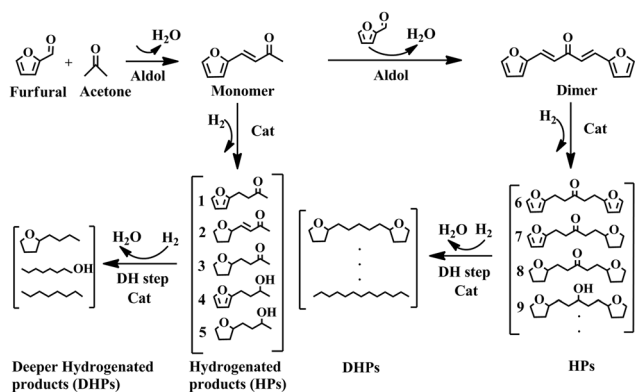
E-mail: chemwy@zju.edu.cn; Fax: (+86)-571-8795-1895

†Electronic supplementary information (ESI) available: Detailed experimental procedures, Fig. S1–S10 and Tables S1–S4. See DOI: 10.1039/c4gc00850b

and water dispersibility compared to carbon-based materials. Attractively, we envision that if it is hybridized in an appropriate manner, a bifunctional catalyst with enhanced properties can be formed which retains its advantages but discards its deficiencies.

Recent years have witnessed an increasing interest in developing renewable energy resources as alternatives to the diminishing supply of non-renewable fossil fuels. Carbohydrates constitute the largest fraction of biomass feedstock, and they can be converted into various platform molecules from which tailor-made products can be achieved through specific catalytic steps. Among the various intermediates are 5-hydroxymethylfurfural (HMF) and furfural (FF), which are accessible from saccharides (a common component of biomass) like glucose, fructose and cellulose.^{35,36} A series of intermediates and final products with extended carbon chains can be obtained through the aldol condensation of FF and acetone followed by hydrogenation steps (Scheme 1). Selective hydrogenation of the monomer and dimer aldol products (Scheme 1) produces increasingly saturated hydrogenated products (HPs) 1–9, and deeper hydrogenation of the HPs produces the corresponding saturated alcohols or even alkanes (deeper hydrogenated products, DHPs).^{2,37} In particular, the intermediates 3 and 8 are of great importance as they offer various options for further derivatization owing to the remaining carbonyl functional group. However, the carbonyl groups tend to be hydrogenated to alcohols (5 and 9), depending on factors such as the solvent, the partial pressure of hydrogen, and the nature of the catalyst. Hence a bifunctional catalyst that is catalytically active for the two tandem steps yet allows the isolation of final products 3 and 8 with high selectivity is desirable.

Herein, we have developed a bifunctional catalyst Pd/CN@MgO, in which the support is composed of uniformly hybridized CN (nitrogen-containing carbon) and MgO, and the deposited Pd was finely dispersed. The application of this catalyst in the tandem aldol condensation–hydrogenation of furfural with acetone demonstrated excellent catalytic activity and high selectivity for the final hydrogenation products 3 and 8. Notably, DHPs were not produced in the present study.



Scheme 1 Reaction network for the tandem reactions of furfural: aldol condensation and the following possible reaction paths of hydrogenation steps.

Experimental

Materials

PdCl₂ (59–60 wt%), D(+)-glucosamine hydrochloride (99%), magnesium oxide (50 nm, spherical, 99.9% metals basis) and furfural (AR, 99%) were used as received from Aladdin Chemistry Co., Ltd. NaBH₄ (96%) and acetone (AR) were used as received from Sinopharm Chemical Reagent Co., Ltd. All solvents and chemicals were used without further treatment.

Synthesis method

In a typical synthesis of 5% Pd/CN@MgO catalyst, 2.0 g glucosamine hydrochloride (GAH) and 0.5 g MgO nanoparticles were thoroughly mixed together in a crucible and heated at 80 °C with stirring to evaporate the added water. The mixture was then calcined under N₂ flow (400 mL min^{−1}) at the programmed temperature of 1000 °C for 1 h, after which it was cooled down to room temperature. Black powder CN@MgO was thus obtained as a catalyst support. Then, 0.2 g CN@MgO and 2 mL of 0.01 g mL^{−1} PdCl₂ solution were mixed well in 20 mL deionized water under ultrasound treatment. 10 mL of a newly prepared NaBH₄ solution (1 mg mL^{−1}) was added to the resulting solution to obtain a ~5% Pd loading. The resultant product was filtered and washed with deionized water several times, and after a drying process, the desired Pd/CN@MgO catalyst was ready to be used. In addition, Pd/CN, Pd/MgO and Pd/(MgO + CN) catalysts were synthesized for comparison by the same method, except that the catalyst supports were varied.

Catalytic reactions

In a typical tandem aldol condensation–hydrogenation reaction of furfural with acetone, 40 mL H₂O was thoroughly mixed with 20 mg Pd/CN@MgO, 0.31 g furfural and 1.69 g acetone, and added into a 150 mL stainless-steel autoclave. The mixture was stirred for 1 h at 120 °C under 0.1 MPa N₂ for the aldol condensation step, followed by a hydrogenation step, in which the mixture was stirred for 3 h at 120 °C under 1.0 MPa H₂. When the above reaction was over and cooled down, the remaining H₂ was removed by a careful venting process, and the reaction mixture was extracted with ethyl acetate (~40 mL). The product distribution was analyzed by GC.

Analytical methods and characterization

The BET specific area was measured on a surface area and porosity analyzer (Micromeritics, ASAP 2020 HD88). Transmission electron microscopy (TEM) was carried out with a Hitachi HT-7700 microscope at an acceleration voltage of 100 kV. High-resolution TEM (HRTEM), Scanning Transmission Electron Microscopy-High Angle Annular Dark Field (STEM-HAADF) and Scanning Transmission Electron Microscopy-Energy Dispersive X-ray (STEM-EDX) were performed on a Tecnai G2 F30 S-Twin at an acceleration voltage of 300 kV. X-Ray powder diffraction (XRD) patterns were measured on a Bruker D8 diffractometer equipped with a scintillation counter. Elemental analyses were obtained on a Vario El elemental analyser. The Pd dispersion was measured on a CHEMBET-3000 apparatus (Quantachrome

Co.). Temperature programmed desorption of CO₂ (CO₂-TPD) was performed on a TPD apparatus equipped with a thermal conductivity detector (TCD). The Pd contents were measured by inductively coupled plasma (ICP) analysis and nitric acid (70 wt%, semiconductor grade) was used to dissolve the sample. The FT-IR spectrum was collected on a Nicolet Nexus 470. The contents of products and substrate were determined by Gas Chromatography-Flame Ionization Detector (GC-FID) (Shimadzu, GC-2014) and the products were identified by Gas Chromatography-Mass Spectrometer (GC-MS) (Agilent Technologies, GC 6890N, MS 5970). Thermogravimetric analyses (TGA) were conducted on a Thermogravimetric Analyzer (TGA 7, PERKIN ELMER). Raman spectra were measured on a Raman spectrometer (JY, HR-800) using a 514 nm laser. The optical contact angles with water were obtained on an interface tension meter (Kino SL 200KB).

Results and discussion

In the present study, a bifunctional catalyst Pd/CN@MgO was obtained through a simple ultrasound-assisted reduction technique.³⁸ The CN@MgO hybrid with N-containing carbon and MgO was prepared through a drying procedure on a mixture of glucosamine hydrochloride (GAH) and MgO, followed by a thermal condensation process. As expected, the as-obtained Pd/CN@MgO exhibited the basicity of MgO, a uniformly small Pd particle size (2.2 nm in average size) with fine dispersion, and excellent water dispersibility and reaction stability. These factors greatly improved the catalytic activity in our present study towards a tandem reaction that combines aldol condensation and selective hydrogenation of a bioderived compound.

Elemental analysis showed that the resulting CN@MgO hybrid had a N/C atom ratio of 0.041 in the carbonaceous part (Table S1†), which is an indication of successfully doping nitrogen into the carbon (4.56% of nitrogen in mass proportion). Thermogravimetric analysis (TGA) of CN@MgO under O₂ flow revealed that the mass ratio of MgO in CN@MgO is ~40.0% (Fig. S2†). The Raman spectra of the prepared CN@MgO and CN (Fig. 1A) shows the characteristic D and G bands of amorphous carbon or disordered graphite with a similar I_D/I_G (I_D represents the intensity of the D band, and I_G represents the intensity of the G band) ratio of ~1.0. This indicates that the carbonaceous part of CN@MgO maintains a very similar graphitic structure to that of N-containing carbon.¹⁰ The X-Ray diffraction (XRD) pattern (Fig. 1B) of

Pd/CN@MgO shows a relatively weak diffraction peak at ~26° which corresponds to graphitic carbon, and diffraction peaks of Pd (111) and Pd (200) at ~40° and ~46° were observed. Strong and sharp MgO peaks were also observed. Exact diffraction data for the MgO are in good agreement with crystalline MgO (PDF# 65-0476).

The high-resolution TEM (HRTEM), STEM-HAADF and STEM-EDX images of the synthesized Pd/CN@MgO catalyst are shown in Fig. 2. The difficulty in synthesizing supported Pd NPs with small size and uniform dispersion means that capping or stabilizing agents are often used^{39,40} which affects catalytic activity and complicates the preparation process, and thus easy methods of synthesizing clean, small and uniformly dispersed supported Pd NPs are desirable. Attractively, our simple ultrasound-assisted reduction technique to deposit Pd on the CN@MgO support gave a uniform dispersion of Pd NPs (Fig. 2A and S3†) with an average particle size of 2.2 nm (inset in Fig. 2A). Inspired by the obtained small Pd NPs with narrow size distribution, the dispersion (D), *i.e.*, the fraction of exposed Pd in the catalyst was further determined by CO chemisorption. The D value for Pd/CN@MgO was determined to be 34%, suggesting a large number of active Pd atoms for

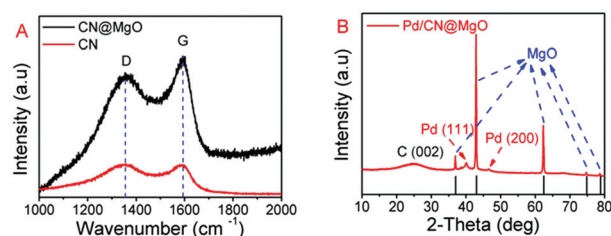


Fig. 1 (A) Raman spectra of CN@MgO and CN; (B) XRD patterns of the synthesized Pd/CN@MgO catalyst.

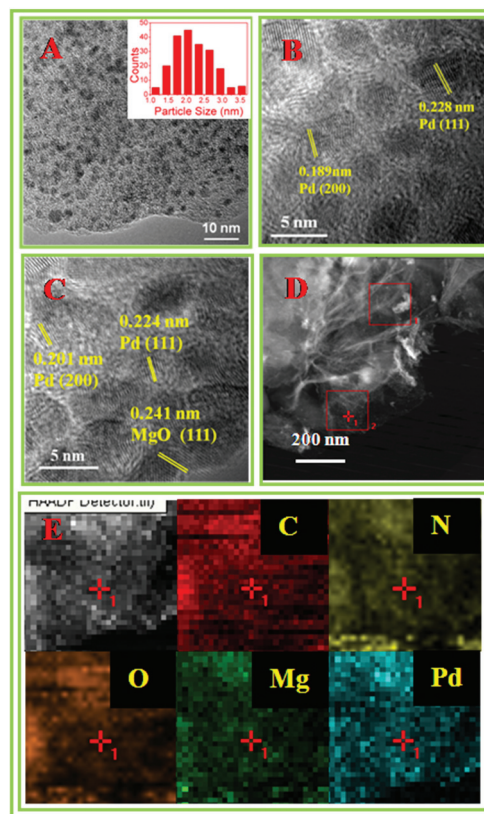


Fig. 2 (A) HRTEM image showing the uniform distribution of Pd NPs with the particle size distribution of Pd NPs for ~200 particles of the Pd/CN@MgO nanocomposite (in the inset); (B) HRTEM image displaying the crystal planes of the surface Pd NPs; (C) HRTEM image clearly showing the amorphous morphology of the carbon coating with a uniform distribution of Pd nanoparticles (NPs); (D) a STEM HAADF image and (E) EDS maps of carbon, nitrogen, oxygen, magnesium and palladium of Pd/CN@MgO.

H₂ chemisorption and activation, thus a high catalytic activity for hydrogenation was expected. The HRTEM image in Fig. 2B revealed two kinds of crystal planes of Pd, and the crystal plane spacings were measured to be 0.224 and 0.198 nm. Considering the structure of the hybrid support composed of MgO and N-doped carbon, we concluded that the MgO was uniformly hybridized with the carbon, as only local exposed MgO crystal lattice sites on the edge of the material were observed in the HRTEM images of Pd/CN@MgO even at high magnifications (Fig. 2C). STEM-HAADF and STEM-EDX were performed to verify the existence of MgO and nitrogen in the nanocomposites (Fig. 2D and 2E). Therefore, the HRTEM, Raman, and XRD investigations indicate that the Pd/CN@MgO hybrid material is composed of basic MgO uniformly hybridized with N-containing carbon, with perfectly dispersed Pd NPs. Thus we envisioned that it may possess some interesting catalytic properties.

For comparison, a series of supports (CN, MgO, and CN + MgO) were prepared to compare their aldol condensation ability with that of CN@MgO. As shown in Table 1, CN alone showed no aldol catalytic ability, primarily due to its weak basicity. Interestingly, CN@MgO displayed the best catalytic activity for aldol condensation at 80 °C for 3 h under a N₂ atmosphere, achieving ~99% furfural conversion. The better condensation activity of the CN@MgO was due to the following factors: (1) the basicity was maintained because of the MgO component in the CN@MgO; (2) a good dispersion of the hybrid in the reaction solutions was achieved by introducing the hydrophilic N-containing carbon¹⁰ (Fig. S4A†); (3) the lower specific gravity of carbon materials compared to MgO, which also enables the hybrid to better disperse in water (Fig. S4B†); (4) the porous structure of the carbon surrounding the MgO matrix (Table S2†). Furthermore, CO₂-TPD investigations of the catalyst supports proved that the MgO in the CN@MgO hybrid may have endowed the surrounding CN with new active sites for aldol condensation (Fig. S5†). These outstanding features of the hybrid catalyst thus improved the exposure of the active sites toward the substrates (furfural and acetone) and enhanced the catalytic performance significantly. We then deposited Pd NPs onto the CN@MgO to form a bifunctional Pd/CN@MgO catalyst, in order to investigate its enhanced catalytic activity, combining both aldol conden-

sation and hydrogenation in a one-pot reactor to simplify the reaction steps. Also, for comparison, the series of catalysts Pd/MgO, Pd/CN and Pd/(MgO + CN) were all synthesized through the simple ultrasound-assisted reduction technique. Theoretically, all of the synthesized Pd catalysts contained 5.66 wt% Pd in mass ratio, and the actual Pd loading by ICP analysis was found to be 4.6%, 6.0%, 5.4% and 5.6% for Pd/CN, Pd/MgO, Pd/(MgO + CN) and Pd/CN@MgO, respectively.

Table 2 gives an overview of the catalytic systems in our study. Unsurprisingly, Pd/CN@MgO showed the best catalytic activity towards the aldol reaction with ~99% furfural conversion, much higher than that of both Pd/MgO and Pd/(MgO + CN), demonstrating that after the addition of Pd NPs the catalytic condensation activity was unaffected. In addition, the Pd/MgO and Pd/(MgO + CN) catalysts gave relatively broad product mixtures while Pd/CN@MgO exhibited a better selectivity towards the products 3 and 8. This indicates that variation of the catalyst support can control the selectivity. That is to say, the simple physical mixture of CN and MgO was incapable of achieving a higher catalytic activity than Pd/CN@MgO, which was more favorable for the aldol reaction. As observed from the TEM images in Fig. 2A and S3,† Pd/CN@MgO had a small Pd size with a narrow size distribution, totally unlike the obvious aggregation of the Pd NPs in Pd/(CN + MgO) (Fig. S6†), and with a much smaller Pd size (~4.9 nm) than the previously reported Pd@CN_{0.132} catalyst with N-doped carbon alone as a support (Fig. S7†).¹⁰ This demonstrates the synergic effect of the two components of the CN@MgO hybrid towards optimizing the anchored Pd NPs. Additionally, the hydrophilicity of the Pd/CN@MgO in the reaction media strengthened its exposure to the substrates, so increased catalytic performance was obtained. Furthermore, the BET specific areas of Pd/MgO, Pd/(CN + MgO) and Pd/CN@MgO were 44, 106 and 172 m² g⁻¹, respectively (see Table 3 for the relevant calculated constants and Fig. S8† for the adsorption/desorption isotherms), which were also in accordance with the total catalytic activity. Therefore, these results strongly suggest that the Pd/CN@MgO nanocomposite could be used as the desired bifunctional catalyst to

Table 1 Aldol condensation of furfural with acetone using different catalyst supports^a

Entry	Cat.	Conv. (%)	Sel. (%)		
			Monomer	Dimer	Others
1	CN	0	0	0	0
2	MgO	87	86	14	0
3	CN + MgO	89	84	15	1
4	CN@MgO	>99	87	12	1

^a Reactions were carried under 0.1 MPa N₂ at 80 °C for 3 h; All runs were carried out in 40 mL H₂O with *c*(furfural) = 0.081 mol L⁻¹ while keeping the molar ratio of furfural-acetone at 1 : 9 and the mass ratio of organic : catalyst at 100 : 1.

Table 2 Catalytic products of tandem aldol condensation-hydrogenation of furfural with acetone by Pd supported catalysts

Entry	Cat. ^a	Conv. ^b (%)	Sel. ^c (%)			
			1	3	7	8
1	Pd/CN	0	0	0	0	0
2 ^d	Pd/MgO	86	39	42	5	6
3	Pd/(CN + MgO)	74	12	77	0	11
4	Pd/CN@MgO	>99	0	82 (2)	0	14 (2)

^a Theoretically synthesized with 5.66 wt% Pd in mass ratio. ^b Furfural conversion in the aldol condensation. ^c Product distribution in the hydrogenation process. ^d Other products (8%) were detected. All runs were carried out in 40 mL H₂O with *c*(furfural) = 0.081 mol L⁻¹ while keeping the molar ratio of furfural-acetone at 1 : 9 and the mass ratio of organic : catalyst at 100 : 1. Condensation was carried out in 0.1 MPa N₂ at 80 °C for 3 h; hydrogenation was carried out in 1.7 MPa H₂ at 120 °C for 3 h. The yields of the corresponding alcohols are shown in brackets.

Table 3 BET specific area, pore volume and average pore size of the catalysts determined by nitrogen sorption measurements

Entry	Catalyst	S_{BET} ($\text{m}^2 \text{g}^{-1}$)	Pore volume ($\text{cm}^3 \text{g}^{-1}$)	Average pore size (nm)
1	Pd/MgO	44	0.22	20
2	Pd/(CN + MgO)	106	0.28	10
3	Pd/CN@MgO	172	0.29	7

further optimize its reaction conditions in order to maximize the formation of our desired products **3** and **8**.

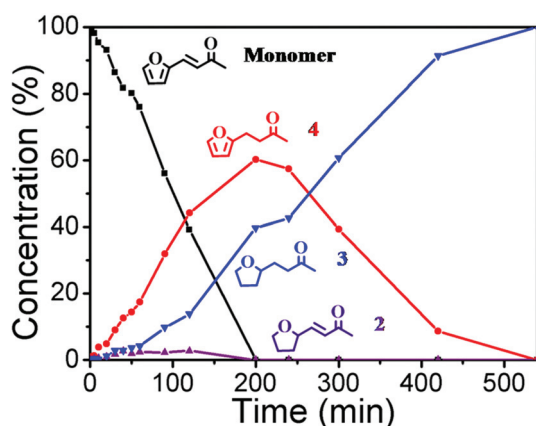
To get a better understanding of the process of gradual hydrogenation of the aldol products by Pd/CN@MgO, the monomer was chosen as a substrate and the reaction was monitored by sampling at 60 °C under 0.1 MPa H_2 as a detailed investigation (Fig. 3). At first both the C=C double bond and the heteroaromatic ring of the monomer were hydrogenated but with a faster rate for the C=C double bond, followed by the total hydrogenation of the heteroaromatic ring to transform the unsaturated products to saturated product **3**, with negligible hydrogenation of the C=O double bond (see Fig. S9† for the detailed product identification using GC-MS). The selectivity of Pd/CN@MgO in the hydrogenation of the various functional groups allows us to selectively obtain **3** and **8** as the main products of the reaction in the present study.

Monitoring the hydrogenation process of the monomer gave access to a better understanding of the intermediates and final products in the consecutive reactions. As the present catalytic process includes aldol condensation and hydrogenation steps for the synthesized bifunctional catalyst Pd/CN@MgO, optimized aldol condensation conditions are required to achieve a desired conversion of furfural. Thus, we first studied different reaction parameters for the aldol condensation between furfural and acetone using Pd/CN@MgO. Therefore, the N_2 pressure, molar ratio of the substrates, reaction time and temperature were chosen as the parameters for consideration (Table S3†). When considering both conversion and monomer selectivity, a molar ratio of furfural to acetone of

1 : 9 with excess acetone reacted at 80 °C for 3 h under 0.1 MPa N_2 was able to achieve >99% furfural conversion (entry 2). When the reaction was conducted at 120 °C under 0.1 MPa N_2 , 1 h was enough for >99% furfural conversion while still retaining the monomer selectivity (entry 8), but ~95% conversion was obtained for the further shortened reaction time of 0.5 h (entry 9), so condensation at 120 °C for 1 h under 0.1 MPa N_2 with a furfural-acetone ratio of 1 : 9 was used for sequential investigation into the hydrogenation step in the following studies.

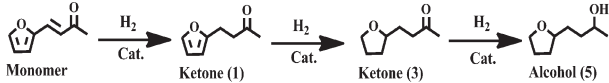
Having optimized the excellent aldol condensation ability of the Pd/CN@MgO catalyst, the following hydrogenation step was investigated that demonstrated its bifunctionality for facilitating a single-reactor, aqueous process that combines aldol condensation with sequential hydrogenation. The hydrogenation of the aldol products (monomer and dimer) results in a series of HPs and DHPs (Scheme 1). Focusing on obtaining the intermediates **3** and **8** with the highest possible selectivity, the hydrogenation conditions of hydrogen pressure, reaction temperature and time were selected for further optimization (Table 4). Obviously, a high target selectivity (**3** and **8**) of 95% can be achieved at 120 °C under 1.0 MPa H_2 (entry 2), and a lower H_2 pressure of 0.5 MPa was not suitable for total conversion to our targets (entry 1). When the temperature was decreased to 100 °C under 1.0 MPa H_2 , a longer time of 5 h was needed for an equal selectivity (entry 3). The results showed that even using 3.0 MPa H_2 for 3 h, product **1** (1%) that was not hydrogenated to **3** was present together with an excess of our hydrogenated products (entry 5). However, when the catalytic hydrogenation was performed at 200 °C under 3.0 MPa H_2 for 15 h, 78% selectivity for the alcohols (**5** and **9**) was obtained (entry 6).

Furthermore, ICP measurements were performed to investigate the loss of Pd from the Pd/CN@MgO under the above reaction conditions. No Pd was detected, suggesting negligible Pd was lost during the tandem reaction process. Recycling experiments for the hydrogenation process proved that the catalyst is highly stable and can be reused several times

**Fig. 3** The evolution of reactant and product selectivity as a function of time using Pd/CN@MgO as a catalyst under 0.1 MPa H_2 at 60 °C.**Table 4** Effects of different parameters for hydrogenation of the aldol condensation products using Pd/CN@MgO

Entry	H_2 (MPa)	Temp. (°C)	Time (h)	Sel. ^a (%)			
				1	3	8	Others
1	0.5	120	3	7	76 (1)	12 (0)	4
2	1.0	120	3	0	84 (1)	11 (1)	3
3	1.0	100	5	1	82 (1)	13 (1)	2
4	2.0	100	5	0	82 (2)	13 (1)	2
5	3.0	100	3	1	80 (3)	13 (2)	1
6	3.0	200	15	0	19 (67)	1 (11)	2

^a Conversion of the hydrogenation process was 100% for all the reactions. The brackets are the corresponding alcohols. All runs were carried out in 40 mL H_2O with $c(\text{furfural}) = 0.081 \text{ mol L}^{-1}$ while keeping the molar ratio of furfural-acetone 1 : 9 and the mass ratio of organic/catalyst 100 : 1, and the hydrogenation reactions were all following the first step of aldol condensation between furfural and acetone in 0.1 MPa N_2 , 120 °C for 1 h as a sequential reaction system.

Table 5 Results of catalyst recycles towards hydrogenation of monomer using Pd/CN@MgO^a


Entry	Recycle runs	Conv. (%)	Sel. (%)		
			3	1	5
1	Fresh	100	98	0	2
2	1 st	100	98	1	1
3	2 nd	100	93	5	2
4	3 rd	100	97	2	1

^a Reaction conditions: monomer 0.1 g, catalyst 40 mg, water 20 mL, H₂ pressure 0.1 MPa, 80 °C, 1.5 h. For each of the recycles, the amount of substrate was reduced in proportion with the recycled catalyst.

without the loss of its catalytic activity (Table 5). These results demonstrate that the deposited Pd NPs are finely anchored on the support, mainly due to the doped nitrogen in the carbon structure which retains the metal NPs.¹⁰ It is known that MgO is easily hydrolyzed to Mg(OH)₂ during hydrothermal treatment, which makes it unstable during reactions in aqueous media. However, in the present study, Pd/CN@MgO demonstrated excellent support stability in the above tandem reaction conditions in water, showing negligible transformation of the MgO into Mg(OH)₂ (Fig. S10A†). This is strong evidence that the carbon structure can also help to stabilize MgO, which also proves that the MgO was uniformly hybridized with carbon (Fig. 2C). However, without the protection and stabilization of the carbon coating, the Pd/MgO catalyst is completely hydrolysed (Fig. S10B†), again illustrating the important function of the carbon structure in the stabilization of the catalyst supports.

Conclusions

In summary, a bifunctional Pd/CN@MgO catalyst was prepared by a very simple ultrasound-assisted reduction technique which can deposit Pd NPs on a bioderived nitrogen-doped carbon coated MgO (CN@MgO) hybrid, and the resulting catalyst contains uniform small Pd NPs with an average size of 2.2 nm and fine dispersion. The introduction of the hydrophilic N-containing carbon structure to the MgO by thermal condensation means that the catalyst also shows both good water dispersion and reaction stability. With such improved features, this catalyst showed high catalytic ability in the tandem aldol condensation–hydrogenation reaction of furfural with acetone in a single reactor, obtaining >99% furfural conversion and 95% hydrogenation products selectivity (84% of 3 and 11% of 8). This bifunctional catalyst opens up a new route for upgrading biomass-derived intermediates and the catalyst design strategy provides a new method for the construction of metal supported bi/multi-functional catalysts with good particle distribution along with improved catalyst hydrophilicity.

Further work will be dedicated to expanding this technique for other metal(s) and support structure modification, with expectations for wider application in other model systems.

Acknowledgements

Financial support from the National Natural Science Foundation of China (21376208 & U1162124), the Zhejiang Provincial Natural Science Foundation for Distinguished Young Scholars of China (LR13B030001), the Specialized Research Fund for the Doctoral Program of Higher Education (J20130060), the Fundamental Research Funds for the Central Universities, the Program for Zhejiang Leading Team of S&T Innovation, the Partner Group Program of the Zhejiang University and the Max-Planck Society are greatly appreciated.

Notes and references

- I. Fechete, Y. Wang and J. C. Védrine, presented in part at the Catal. Today, 2012.
- G. W. Huber, J. N. Chheda, C. J. Barrett and J. A. Dumesic, *Science*, 2005, **308**, 1446–1450.
- X. Huang, C. Guo, J. Zuo, N. Zheng and G. D. Stucky, *Small*, 2009, **5**, 361–365.
- K. Yoon, Y. Yang, P. Lu, D. Wan, H. C. Peng, K. Stamm Masias, P. T. Fanson, C. T. Campbell and Y. Xia, *Angew. Chem., Int. Ed.*, 2012, **51**, 9543–9546.
- S. H. Joo, J. Y. Park, C.-K. Tsung, Y. Yamada, P. Yang and G. A. Somorjai, *Nat. Mater.*, 2009, **8**, 126–131.
- H. Liu, T. Jiang, B. Han, S. Liang and Y. Zhou, *Science*, 2009, **326**, 1250–1252.
- X. Gu, Z.-H. Lu, H.-L. Jiang, T. Akita and Q. Xu, *J. Am. Chem. Soc.*, 2011, **133**, 11822–11825.
- M. Meilikhov, K. Yusenko, D. Esken, S. Turner, G. Van Tendeloo and R. A. Fischer, *Eur. J. Inorg. Chem.*, 2010, **2010**, 3701–3714.
- A. La Torre, M. d. C. Giménez-López, M. W. Fay, G. A. Rance, W. A. Solomonsz, T. W. Chamberlain, P. D. Brown and A. N. Khlobystov, *ACS Nano*, 2012, **6**, 2000–2007.
- X. Xu, Y. Li, Y. Gong, P. Zhang, H. Li and Y. Wang, *J. Am. Chem. Soc.*, 2012, **134**, 16987–16990.
- D. J. Davis, A.-R. O. Raji, T. N. Lambert, J. A. Vigil, L. Li, K. Nan and J. M. Tour, *Electroanalysis*, 2014, **26**, 164–170.
- X. Pan, Z. Fan, W. Chen, Y. Ding, H. Luo and X. Bao, *Nat. Mater.*, 2007, **6**, 507–511.
- J. Kang, S. Zhang, Q. Zhang and Y. Wang, *Angew. Chem., Int. Ed.*, 2009, **48**, 2565–2568.
- P. Zhang, J. Yuan, T. P. Feller, M. Antonietti, H. Li and Y. Wang, *Angew. Chem., Int. Ed.*, 2013, **52**, 6028–6032.
- W. Lin, H. Cheng, J. Ming, Y. Yu and F. Zhao, *J. Catal.*, 2012, **291**, 149–154.
- S. Crossley, J. Faria, M. Shen and D. E. Resasco, *Science*, 2010, **327**, 68–72.

- 17 M. P. Ruiz, J. Faria, M. Shen, S. Drexler, T. Prasomsri and D. E. Resasco, *ChemSusChem*, 2011, **4**, 964–974.
- 18 C. J. Barrett, J. N. Chheda, G. W. Huber and J. A. Dumesic, *Appl. Catal., B*, 2006, **66**, 111–118.
- 19 J. Julis and W. Leitner, *Angew. Chem., Int. Ed.*, 2012, **51**, 8615–8619.
- 20 A. Corma, T. Rodenas and M. J. Sabater, *Chem. – Eur. J.*, 2010, **16**, 254–260.
- 21 B. Peng, Y. Yao, C. Zhao and J. A. Lercher, *Angew. Chem., Int. Ed.*, 2012, **51**, 2072–2075.
- 22 A.-H. Lu, G.-P. Hao, Q. Sun, X.-Q. Zhang and W.-C. Li, *Macromol. Chem. Phys.*, 2012, **213**, 1107–1131.
- 23 Y. Zhai, Y. Dou, D. Zhao, P. F. Fulvio, R. T. Mayes and S. Dai, *Adv. Mater.*, 2011, **23**, 4828–4850.
- 24 B. Hu, K. Wang, L. Wu, S. H. Yu, M. Antonietti and M. M. Titirici, *Adv. Mater.*, 2010, **22**, 813–828.
- 25 L. Zhao, N. Baccile, S. Gross, Y. Zhang, W. Wei, Y. Sun, M. Antonietti and M.-M. Titirici, *Carbon*, 2010, **48**, 3778–3787.
- 26 S. Maldonado and K. J. Stevenson, *J. Phys. Chem. B*, 2005, **109**, 4707–4716.
- 27 L. Zhao, L. Z. Fan, M. Q. Zhou, H. Guan, S. Qiao, M. Antonietti and M. M. Titirici, *Adv. Mater.*, 2010, **22**, 5202–5206.
- 28 Y.-H. Li, T.-H. Hung and C.-W. Chen, *Carbon*, 2009, **47**, 850–855.
- 29 G.-X. Chen, J.-M. Zhang, D.-D. Wang and K.-W. Xu, *Physica B*, 2009, **404**, 4173–4177.
- 30 Z. Li, J. Liu, C. Xia and F. Li, *ACS Catal.*, 2013, **3**, 2440–2448.
- 31 Y. Wang, J. Yao, H. Li, D. Su and M. Antonietti, *J. Am. Chem. Soc.*, 2011, **133**, 2362–2365.
- 32 Y. Gong, P. Zhang, X. Xu, Y. Li, H. Li and Y. Wang, *J. Catal.*, 2013, **297**, 272–280.
- 33 P. Zhang, Y. Gong, H. Li, Z. Chen and Y. Wang, *Nat. Commun.*, 2013, **4**, 1593.
- 34 A. M. Frey, J. Yang, C. Feche, N. Essayem, D. R. Stellwagen, F. Figueras, K. P. de Jong and J. H. Bitter, *J. Catal.*, 2013, **305**, 1–6.
- 35 H. Zhao, J. E. Holladay, H. Brown and Z. C. Zhang, *Science*, 2007, **316**, 1597–1600.
- 36 E. I. Gurbuz, J. M. Gallo, D. M. Alonso, S. G. Wettstein, W. Y. Lim and J. A. Dumesic, *Angew. Chem., Int. Ed.*, 2013, **52**, 1270–1274.
- 37 A. D. Sutton, F. D. Waldie, R. Wu, M. Schlaf, L. A. ‘Pete’ Silks III and J. C. Gordon, *Nat. Chem.*, 2013, **5**, 428–432.
- 38 Y. Li, X. Xu, P. Zhang, Y. Gong, H. Li and Y. Wang, *RSC Adv.*, 2013, **3**, 10973.
- 39 V. Mazumder and S. Sun, *J. Am. Chem. Soc.*, 2009, **131**, 4588–4589.
- 40 J. A. Lopez-Sanchez, N. Dimitratos, C. Hammond, G. L. Brett, L. Kesavan, S. White, P. Miedziak, R. Tiruvalam, R. L. Jenkins, A. F. Carley, D. Knight, C. J. Kiely and G. J. Hutchings, *Nat. Chem.*, 2011, **3**, 551–556.